TECHNICAL NOTE

EFFICIENCY OF ANTI-HOURGLASSING APPROACHES IN FINITE ELEMENT METHOD

G. H. Majzoobi

Faculty of Engineering, Bu- Ali Sina University
Hamadan, Iran

G. H. Farrahi
School of mechanical Engineering, Sharif University of Technology
Tehran, Iran

F. Ferdows Farahani

Faculty of Engineering, Bu- Ali Sina University
Hamadan, Iran

(Received: January 7, 2000 – Accepted in Revised Form:)

Abstract one of the simplest numerical integration method which provides a large saving in computational efforts, is the well known one-point Gauss quadrature which is widely used for 4 nodes quadrilateral elements. On the other hand, the biggest disadvantage to one-point integration is the need to control the zero energy modes, called hourglassing modes, which arise. The efficiency of four different anti-hourglassing approaches, Flanagan (elastic approach), Dyna3d, Hansbo and Liu have been investigated. The first two approaches have been used in 2 and 3-D explicit codes and the latters have been employed in 2-D implicit codes. For 2-D explicit codes, the computational time was reduced by 55% and 60% for elastic and Dyna3d, respectively. However, for 3-D codes the reduction was dependent on the number of elements and was obtained between 50% and 70%. Also, the error due to the application of elastic methods was less than that for Dyna3d when the results were compared with those obtained from 2-points Gauss quadrature. Nevertheless, the convergence occurred more rapidly and the oscillations were damped out more quickly for Dyna3d approach. For implicit codes, the anti-hourglassing methods had no effect on the computations and therefore a 2-points Gauss quadrature is recommended for implicit codes as it provide the results more accurately.

Key Words Hourglassing, Anti-Hourglassing Control, Flanagan Method (Elastic), Dyna3d, Hansbo, Liu, Explicit, Implicit

چکیده

1. INTRODUCTION

One of the most efficient numerical integration in Finite Element is Gauss quadrature. This method is based upon the use of Legendre polynomials and has the minimum points for an optimized integration.

One-dimensional Gauss rule is:

$$\int_{-1}^{+1}\phi(\xi)d\xi=\sum_{i=1}^{n}w_i\phi(\xi_i) \quad (1)$$

In which *n* is the number of integrating points, ξ_i is the value of local coordinate ξ at point i and w_i is the weight of *i*th point. In 2 and 3-dimension, Gauss rules are as follows:

$$\int_{-1}^{1}\int_{-1}^{1}\phi(\xi,\eta)d\xi d\eta=\sum_{i=1}^{n}\sum_{j=1}^{m}w_i w_j\phi(\xi_i,\eta_j) \quad (2)$$

$$\int_{-1}^{1}\int_{-1}^{1}\int_{-1}^{1}\phi(\xi,\eta,\zeta)d\xi d\eta d\zeta=\sum_{i=1}^{n}\sum_{j=1}^{m}\sum_{k=1}^{k}w_i w_j w_k f(\xi_i,\eta_j,\zeta_k) \quad (3)$$

It is evident that one-point Gauss quadrature requires only one iteration for integration, while the number of iterations for 2-D and 3-D problems is 4 and 8 respectively. This implies that the use of one-point Gauss quadrature offers a large saving in computational operations. This is highly important in solving the time dependent finite element problems in which the integration must be repeated at each time step, and also in solving the problems with large number of elements.

However, the use of low-order Gauss quadrature leads to instabilities, which may arise because of shortcomings in the element formulation process. The instability may be called spurious singular mode, kinematics mode, zero energy mode, or hourglass mode. The term "zero energy mode" refers to a nodal displacement vector $\{Q\}$ that is not a rigid-body motion but nevertheless produces zero strain energy.

$$(\tfrac{1}{2}\vec{Q}^{T}[K]\vec{Q})$$

To explain the term "zero energy mode" further and show how such a mode may arise, we substitute the relation and $[K^e]=\int_{V^e}[B]^T[D][B]dV$ and $\{\varepsilon\}=[B]\{\vec{Q}\}^e$ into the expression for strain energy

TABLE 1. Displacement Vectors of a Hexahedron Element.

Node	ξ	η	ζ	Σ_1	Λ_{1I}	Λ_2	Λ_{3I}	Γ_{1I}	Γ_{2I}	Γ_{3I}	Γ_{4I}
1	-1	-1	-1	1	-1	-1	-1	1	1	1	-1
2	1	-1	-1	1	1	-1	-1	1	-1	-1	1
3	1	1	-1	1	1	1	-1	-1	-1	1	-1
4	-1	1	-1	1	-1	1	-1	-1	1	-1	1
5	-1	-1	1	1	-1	-1	1	-1	-1	1	1
6	1	-1	1	1	1	-1	1	-1	1	-1	-1
7	1	1	1	1	1	1	1	1	1	1	1
8	-1	1	1	1	-1	1	1	1	-1	-1	-1

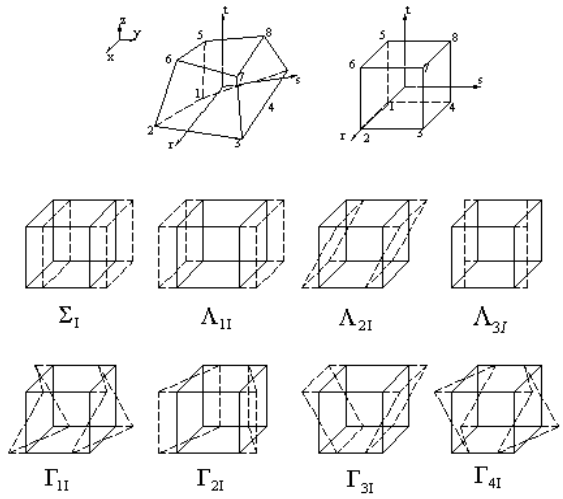

Figure 1. Hexahedron and its displacement.

in an element , U_e :

$$U_e=\tfrac{1}{2}\int_{V_e}\sigma\vec{\varepsilon}dV=\tfrac{1}{2}\int_{V_e}\vec{\varepsilon}^{T}[D]\vec{\varepsilon}dV=\tfrac{1}{2}\vec{Q}^{T}\int_{V_e}[B]^T[D][B]dV\vec{Q}=\tfrac{1}{2}\vec{Q}^{T}[K]\vec{Q} \quad (4)$$

When $[K]$ is formed by numerical integration, it

contains only the information that can be sensed at the sampling points of the quadrature rule. If it happens that $\{\varepsilon\}=[B]\{\bar{Q}\}^e$ are zero at all sampling points for a certain mode, $\{Q\}$then U_e will vanish for that $\{Q\}$ and, according to Equation 4, $[K]$ will be a zero stiffness matrix in the sense that strain energy U_e is zero for this particular $\{Q\}$. We expect that $U_e = 0$ if $\{Q\}$ is a rigid body motion. If U_e is zero when $\{Q\}$ is not a rigid body motion, then an instability is present.

Now, consider a hexahedron element in 3-D space whose stiffness matrix is 8 by 8. The relation for the shape functions of this element can be expressed as follows [1]:

$$N_I = \tfrac{1}{8}(\Sigma_I + \xi\Lambda_{1I} + \eta\Lambda_{2I} + \zeta\Lambda_{3I} + \eta\zeta\Gamma_{1I} + \xi\zeta\Gamma_{2I} + \xi\eta\Gamma_{3I} + \xi\eta\zeta\Gamma_{4I}) \quad (5)$$

In which there are eight independent displacement modes $\{Q\}$ that can be identified as $\Sigma_I, \Lambda_{1I}, \Lambda_{2I}, \Lambda_{3I}, \Gamma_{1I}, \Gamma_{2I}, \Gamma_{3I}$ and Γ_{4I}, and are given in Table 1. These displacement modes are shown in Figure 1.

Similarly, for quadilateral element we have:

$$N_I = \tfrac{1}{4}(\Sigma_I + \xi\Lambda_{1I} + \eta\Lambda_{2I} + \xi\eta\Gamma_I) \quad (6)$$

in which $\Sigma_I, \Lambda_{1I}, \Lambda_{2I}$ and Γ_I are displacement modes of the element and are given in Table 2 .The modes are also shown in Figure 2.

The first one is a rigid body mode, for which $U_e = 0$. The next two modes are constant-strain mode, for which $U_e \rangle 0$. Mode 3 is bending mode. The one-point rule, whose single Gauss point is at the element center, dose not sense this mode, as $\varepsilon_x = \varepsilon_y = \gamma_{xy} = 0$ at the center. The mechanism 3, which corresponds to mode Γ_I is called hourglass mode because of its physical shape.

Though, the savings in cost, which is attributable to one point integration, should not be scarified to prevent hourglassing. Thus, we consider the anti-hourglass control procedures of Flanagan and Belytschko [1], Dyna3d [2], Hansbo [4], and Liu et al [3].

TABLE 2. Displacement Vectors of a Quadilateral Element.

Node	ξ	η	Σ_I	Λ_{1I}	Λ_{2I}	Γ_I
1	-1	-1	1	-1	-1	1
2	1	-1	1	1	-1	-1
3	1	1	1	1	1	1
4	-1	1	1	-1	1	-1

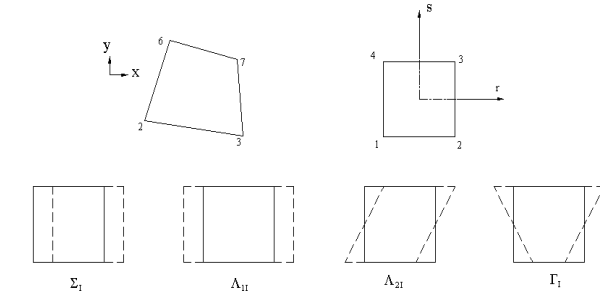

Figure 2. Quadilateral and its displacement modes.

Flanagan and Belytschko have used an artificial load to the nodal forces to combat hourglassing. In their procedure, the hourglass resistance is given as follows:

$$f_{iI}^{HG} = \frac{1}{\sqrt{8}} Q_{i\alpha}\gamma_{\alpha I} \qquad (i = 1 \text{ to } 3) \quad (7)$$

$\gamma_{\alpha I}$ can be calculated using the relation:

$$\gamma_{\alpha I} = \Gamma_{\alpha I} - \frac{1}{V} B_{iI} x_{ij} \Gamma_{\alpha j} \quad (8)$$

In which V is the volume of the element, B_{iI} is geometry matrix and X_{ij} is the nodal coordinates. $Q_{i\alpha}$ is the generalized force, which is

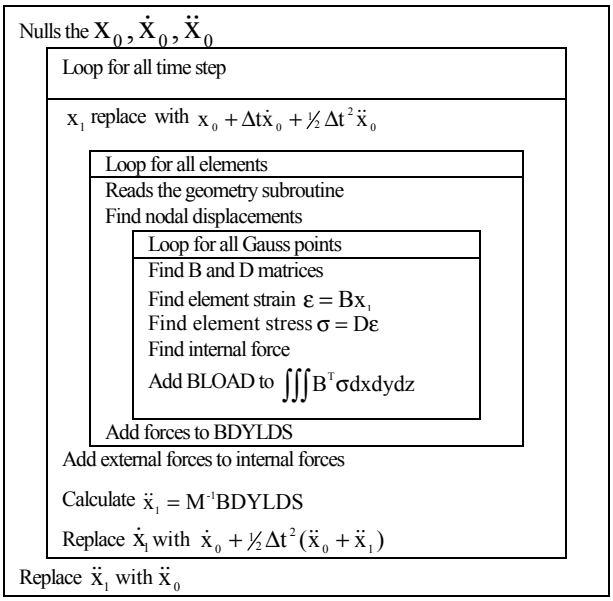

Figure 3. Flow chart of EXPLICIT-3D.

$$\dot{Q}_{i\alpha} = \kappa\frac{\lambda + 2\mu}{3}\frac{B_{iI}B_{iI}}{V}\dot{q}_{i\alpha} \tag{9}$$

$$Q_{i\alpha} = \varepsilon\sqrt{\frac{\rho(\lambda + 2\mu)B_{iI}B_{iI}}{6}}\dot{q}_{i\alpha} \tag{10}$$

For the artificial damping and artificial stiffness, respectively. ε and κ are the user defined damping and stiffness parameters ,respectively. λ and μ are lame' coefficients, and $\dot{q}_{i\alpha}$ is the hourglass modal velocity and is expressed as follows:

$$\dot{q}_{i\alpha} = \frac{1}{\sqrt{8}}\dot{u}_{iI}\gamma_{\alpha I} \tag{11}$$

Where $\dot{u}_{iI}$ is the nodal velocity.

Lawrence Livermore national laboratory has employed another hourglass control scheme which is used in Dyna3d F.E. code. In this method a viscous hourglass resisting force is calculated from the relation [2]:

$$f_{iI} = -a_h\sum_{j=1}^{4}h_{i\alpha}\Gamma_{\alpha I}, (i = 1,3) \tag{12}$$

Where $h_{i\alpha}$ defines the magnitude of the hourglass mode $h_{i\alpha} = \sum_{k=1}^{8}v_i^I\Gamma_{\alpha I}$ and $a_h = Q_{hg}\rho V^{2/3}c/4$, in which V_e is the element volume, c is the material sound speed, Q_{hg} is a user defined constant usually set to a value between 0.05 and 0.15, v_i^k is the nodal velocity of the kth node in ith direction.

Hansbo has proposed a method of quadrature for bilinear element, which may be interpreted as one-point Gaussian quadrature with stabilizing hourglass control. In this method, one way of increasing the accuracy of a quadrature scheme without increasing the number of evaluation points is to use both functional evaluation and evaluation of derivatives, i.e.

$$\int_{-1}^{1}\int_{-1}^{1}f(\xi,\eta)drds \approx W_1 f(0,0) + W_2\left(\frac{\partial^2 f}{\partial\xi^2}(0,0) + \frac{\partial^2 f}{\partial\eta^2}(0,0)\right) \tag{13}$$

In which w_1 and w_2 are 4 and $2/3$, respectively. In the proposed method, the stiffness matrix is calculated as follows:

$$K_{ij} = \int_{-1-1}^{1}\int^{1}(\nabla N_i)_0^T J_0^{-T}\varepsilon_0 J_0^{-1}(\nabla N_i)_0^T \det J_0 d\xi d\eta = \int B^T DBd\xi d\eta \tag{14}$$

In which the subscript 0 indicates the value of the parameter at element center $(\xi = \eta = 0)$ and ε is a constant usually set to one. The integration should be done using Equation 13.

Liu et al [3] have proposed a different technique to combat hourglassing. In their proposed method, a stabilizing stiffness matrix K^s is added to the stiffness matrix obtained from one-point Gauss quadrature $[K^1]$ to vanish the hourglass modes:

$$K_{ij}^S = \tfrac{1}{3}AB_{i,\xi}^T(0)DB_{j,\xi}(0) + \tfrac{1}{3}AB_{i,\eta}^T(0)DB_{j,\eta}(0) \tag{15}$$

In which A is the element area and D is the property matrix. Similarly, for 3-dimension, the Equation 15

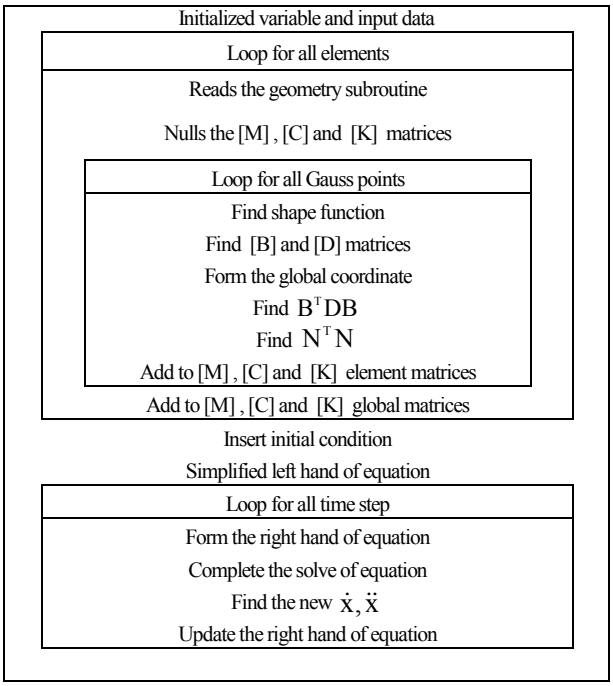

Figure 4. Flow chart of IMPLICIT-2D.

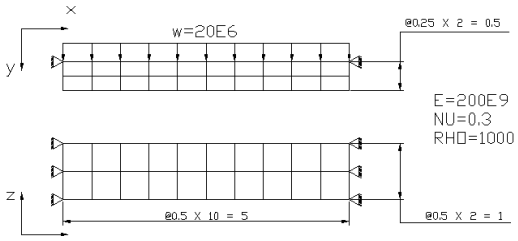

Figure 5. 3-D example.

becomes:

$$K_{ij}^{S} = \frac{1}{3}VB_{i,\xi}^{T}(0)DB_{j,\xi}(0) + \frac{1}{3}AB_{i,\eta}^{T}(0)DB_{j,\eta}(0) + \frac{1}{3}AB_{i,\zeta}^{T}(0)DB_{j,\zeta}(0) + \frac{4}{9}VB_{i,\xi\eta}^{T}(0)DB_{j,\xi\eta}(0) + \frac{4}{9}VB_{i,\eta\zeta}^{T}(0)DB_{j,\eta\zeta}(0) + \frac{4}{9}VB_{i,\zeta\eta}^{T}(0)DB_{j,\zeta\eta}(0) \quad (16)$$

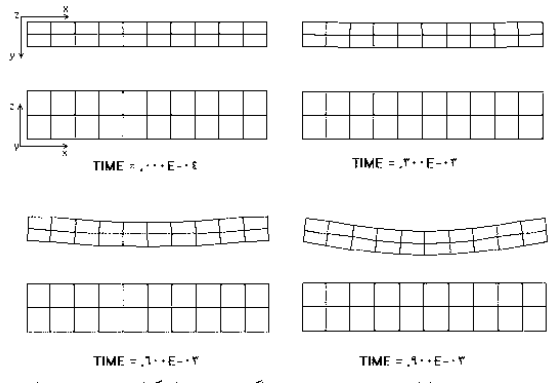

Figure 6. Sequence of the deformed shape of the beam obtained using 2-point Gauss integration.

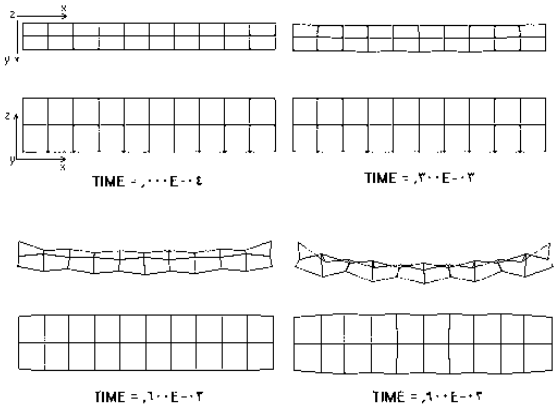

Figure 7. Sequence of the deformed shape of the beam obtained using 1-point Gauss integration without anti-hourglass control.

In which V is the element volume.

2. COMPUTER PROGRAMS

In order to asses the efficiency of the previously mentioned anti-hourglass control procedures, two 2-D and 3-D explicit and 2-D implicit computer programs are written in Fortran 90 for solving time dependent elastic problems. The first program called "EXPLICIT-3D" employs isoparametric hexahedron elements with three degrees of freedom at each node. The second program named "EXPLICIT-

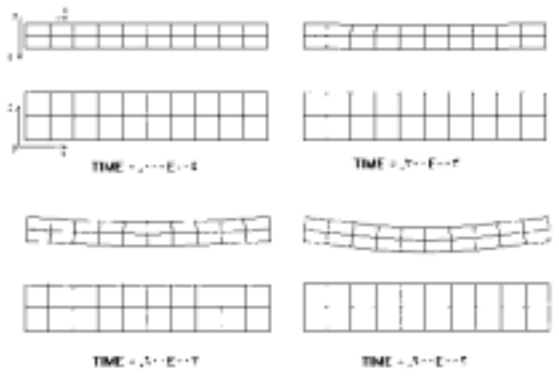

Figure 8. Sequence of the deformed shape of the beam obtained using 1-point Gauss integration with Elastic anti-hourglass control.

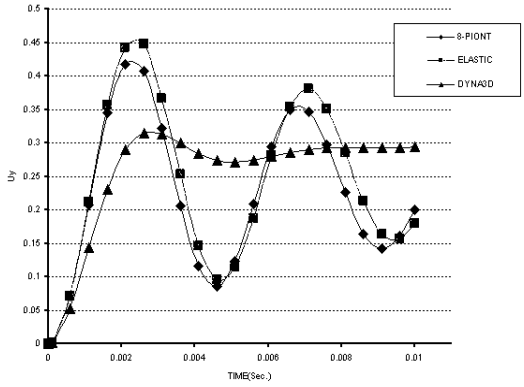

Figure 10. The time-history of midpoint displacement of the beam.

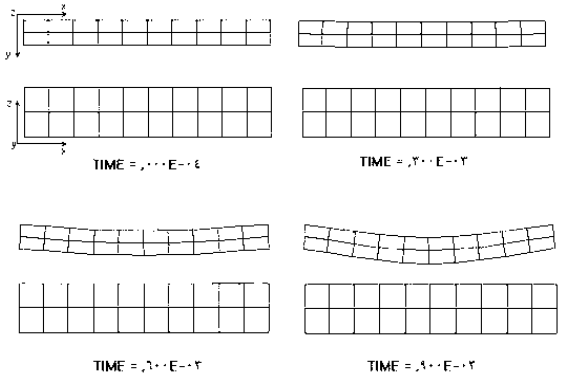

Figure 9. Sequence of the deformed shape of the beam obtained using 1-point Gauss integration with Dyna3d anti-hourglass control.

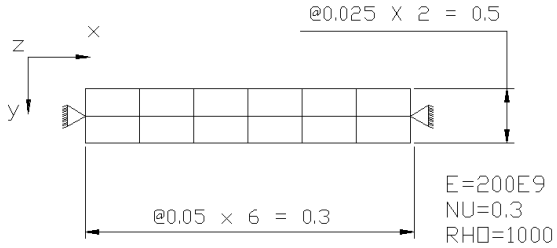

Figure 11. 2-D example

2D" uses isoparametric quadilateral element with two degrees of freedom at each node. Lump mass matrices have been used in both programs. The steps of the solution (flow chart) in EXPLICIT-3D and EXPLICIT-2D are shown in Figure 3. Two optional anti-hourglass schemes, Elastic and Dyna3d, have been incorporated in the programs.

The third program called "IMPLICIT-2D" was allocated to the solution of two-dimensional elastic and time dependent plain strain problems. Two anti-hourglass approaches, Hansbo and Liu, were incorporated in the program to investigate the efficiency of the approaches in implicit codes. The flow chart of IMPLICIT-2D is shown in Figure 4.

3. NUMERICAL RESULTS

Example 1 The first example is a 3-D simply supported rectangular beam, which is subjected to a uniform distributed loading. The numerical simulation has been carried out using EXPLICIT-3D. The dimensions of the beam and its properties are given in Figure 5. In Figure 6, the deformed shape of the beam obtained using 2-point Gauss integration is shown and Figures 7 to 9 illustrate the solution with no anti-hourglass control, Elastic

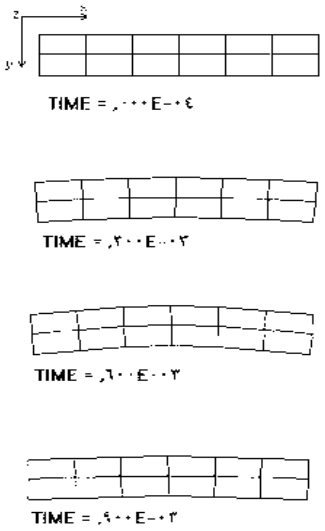

Figure 12. Sequence of the deformed shape of the beam obtained using 2-point Gauss integration.

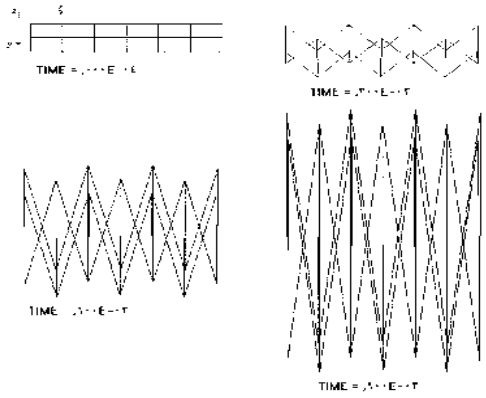

Figure 13. Sequence of the deformed shape of the beam obtained using 1-point Gauss integration without anti-hourglass control.

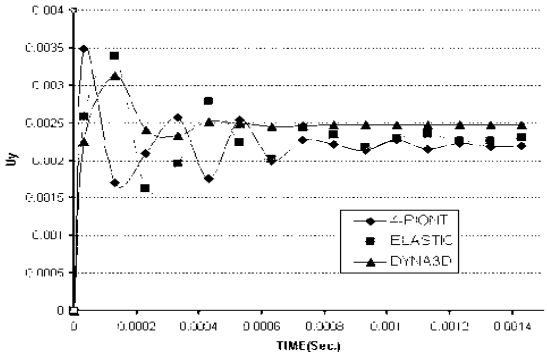

Figure 14. The time-history of midpoint displacement of the beam.

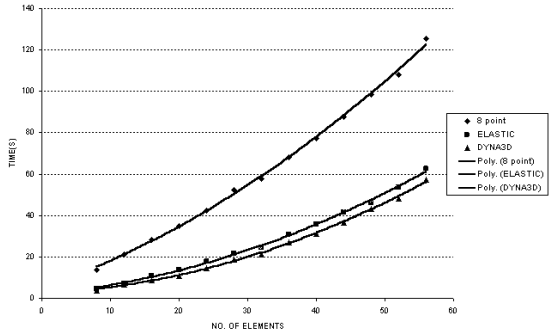

Figure 15. Variation of CPU-time versus the number of elements for EXPLICIT-3D program.

control, and Dyna3d control, respectively. Figure 7 indicates that the use of one-point Gauss quadrature results in a gross mesh distortion, which is caused by the unstable global mode. Consequently, the solution rapidly becomes meaningless. The solution for anti-hourglass Elastic and Dyna3d methods are shown in Figures 8 and 9 respectively. Figure 8 demonstrates that the anti-hourglass stiffness κ = 0.125 stabilizes the solution. This value of κ, suggested by Flanagan and Belytschko [1], has been chosen so that the hourglass mode in the x-direction is integrated as accurately as possible. Flanagan and Belytschko have shown that by increasing the value of κ even by several times, the solution would not be affected significantly. Figure 9 illustrates that Dyna3d has stabilized the solution for $Q_{hg} = 0.1$. This value is the default value defined in Dyna3d hydrocode [8]. However, the Figures 8 and 9 don't represent any difference

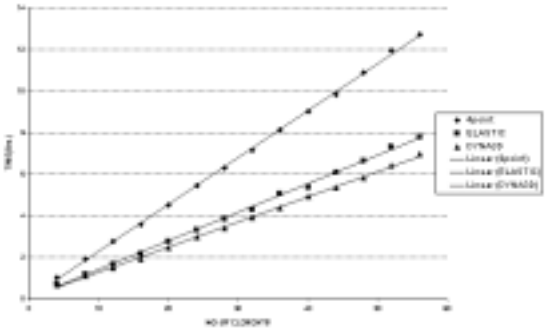

Figure 16. Variation of CPU-time versus the number of elements for EXPLICIT-2D program.

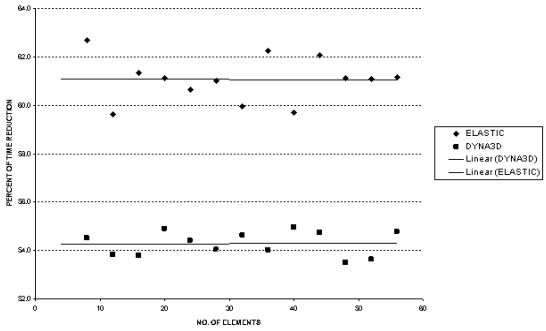

Figure 18. Variation of CPU-time reduction for EXPLICIT-2D program.

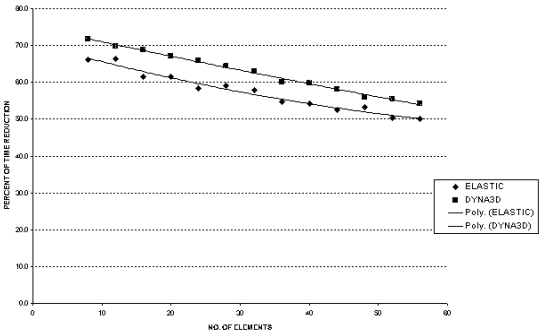

Figure 17. Variation of CPU-time reduction for EXPLICIT-3D program.

between the two anti-hourglass control schemes. Therefore, in order to study the efficiency of the methods more accurately, the time-history of midpoint displacement of the beam was obtained Figure 10 shows the displacement of midpoint; obtained using 2-point Gauss quadrature and anti-hourglass schemes, Elastic and Dyna3d. The figure demonstrates that the Elastic anti-hourglass slows down the oscillations of displacement but dues not stabilize the solution, while Dyna3d method rapidly damps out the oscillations and stabilizes the solution within a short period of time. A comparison also can be made for the maximum deflection of midpoint of the beam (y_{max}) obtained from the exact solution with those obtained from the numerical simulations. y_{max} for a simply supported beam with a uniform distributed load is calculated from the relation:

$$y_{max} = \frac{5wl^4}{384EI} \qquad (17)$$

For the data shown in Figure 5 we obtain $y_{max} = 0.26$. From Figure 10, the midpoint maximum deflection is found to be 0.27, 0.28 and 0.29 for two-point integration, Elastic and Dyna3d anti-hourglass schemes, respectively. Therefore, a good agreement between the exact and the numerical solution is obtained.

Example 2 The second example is a 2-D beam with simply supported ends. It is subjected to a concentrated loading. The numerical simulation has been performed using EXPLICIT-2D. The geometry and properties of the beam is shown in the Figure 11. In Figure 12 the solution has been shown for 4-point integration and Figure 13 illustrates the solution with no anti-hourglass control. Figure 13 shows the gross mesh distortion caused by the unstable global mode. Obviously, the solution

rapidly becomes meaningless. Observe also that an unrestrained global mode persists even though the elements hourglass mode shapes change drastically. In other word, mesh dose not stabilizes as it distorts. The solutions with Elastic and Dyna3d anti-hourglass schemes, not shown here, indicated that a value of $\kappa = 0.125$ for Elastic method and $Q_{hg} = 0.1$ for Dyna3d scheme could prevent hourglass modes to happen. Here again, the theoretical midpoint displacement of the beam (y_{max}) was compared with those obtained from the numerical simulations. y_{max} for a simply supported beam with a concentrated load F at its center is calculated from the relation:

$$y_{max} = \frac{Fl^3}{48EI} \qquad (18)$$

For the data shown in Figure 11 we obtain $y_{max} = 0.0021\text{m}$. Figure 14 shows the time-history of midpoint displacement of the beam. Again, it is observed that, oscillations are damped out more rapidly for Dyna3d method compared with Elastic method and even 4-point integration rule. A comparison between the theoretical value of midpoint displacement with those obtained from the Elastic and Dyna3d methods is given in Table 3. As it is seen, an error of about 9.5% and 19% obtained for Elastic and Dyna3d anti-hourglass scheme, respectively.

The numerical modeling with different number of elements were performed on a Pentium III PC and the CPU time was measured for 1000 time steps. The results are shown in Figures 15 and 16 for EXPLICIT-3D and EXPLICIT-2D, respectively. As it is seen, the numerical modeling have been carried out for 2-point integration, Elastic and Dyna3d anti-hourglass schemes. From Figures 15 and 16, the reduction in CPU-time for Elastic and Dyna3d methods with respect to that for 2-point integration for each number of element was calculated. The results are shown in Figures 17 and 18. It is observed that, for the 2-D explicit code, the computational time is reduced by 55% and 60% for Elastic and Dyna3d, respectively. However, for the 3-D explicit code, the reduction is depends on the number of elements and is obtained between 50% and 70%.

TABLE 3. Comparison Between the Theoretical Value of Midpoint Displacement With Those Obtained From the Elastic and Dyna3d Methods.

No. of example	Theoretical solution	Finite elements method					
		2-point Gauss quadrature quadrature		One-point Gauss quadrature			
				Elastic method		Dyna3d method	
		Ans.	Err. %	Ans.	Err. %	Ans.	Err. %
1	0.25	0.27	3.8	0.28	7.6	0.29	11.4
2	0.0021	0.0022	4.7	0.0023	9.5	0.0025	19

4. CONCLUSION

From the previous result and discussion the following conclusion can be derived:

1- 8-point integration for 3-D problems and 4-point integration for 2-D problems provides the solution more accurately than one-point Gauss quadrature that produces a global unstable deformation mode called hourglassing.

2- Dyna3d anti-hourglass scheme stabilize the solution more rapidly than Elastic methods. However, both methods can successfully vanish the hourglassing deformation.

3- A large saving in computational efforts is achieved for one-point integration rule when using anti-hourglass Elastic and Dyna3d procedures.

4- For implicit methods, anti-hourglass schemes have no effect on computations. So, two-point integration rule will be to the benefit in this case as it predicts the solution more accurately.

5- If there is some constraints that may prevent the hourglassing to happen, then by taking some precautions, anti-hourglass procedures can be omitted from the program. This will results in more saving in computational operations.

5. ACKNOWLEDGEMENT

The another's would like to thank Dr. Nili. The dean of faculty, for his support specially for having prepared computer facilities for this research.

6. REFERENCE

1. Flanagan, D. P. and Belytschko, T., "A Uniform Strain Hexahedron and Quadilateral With Orthogonal Hourglass Control", ***Int. J. Numer. Methods Engrg.***, 17, (1981), 679-706.
2. Hallquist, J. O., "Theoretical Manual for DYNA3d", Lawrence Livermore National Laboratory, March (1983).
3. Liu, W. K, Ong, J, S.-J. and Uras, R. A., "Finite Element Stabilization Matrices-A Unification Approach", ***Comput. Methods Appl. Mech. Engrg.***, 53, (1985), 13-46.
4. Hansbo, P., "A New Approach to Quadrature for Finite Elements Incorporating Hourglass Control Especial Case", ***Comput. Methods Appl. Mech. Engrg.***, 158, (1998), 301-309.
5. Cook, R. D., "Concept and Application of Finite Element Analysis", (Third Edition), John Wiley, New York, (1989).
6. Hughes, T. J. R., "The Finite Element Method", Prentice-Hall Inc., (1987).
7. Smith, I. M. and Griffiths, D. V., "Programming the Finite Element Method", (third edition), John Wiley, New York, (1997).
8. Hallquist, J. O., "User Manual for DYNA3d", Lawrence Livermore National Laboratory, March (1983).